

COLOR TRANSFORMATIONS FOR LOSSLESS IMAGE COMPRESSION

Marek Domański, Krzysztof Rakowski

Poznań University of Technology, Institute of Electronic and Telecommunications,
Piotrowo 3A, 60-965, Poznań, POLAND.

Tel: +48 61 66 52 171, +48 61 66 52 762, fax: +48 61 66 52 572

e-mail: {domanski, krakos}@et.put.poznan.pl

ABSTRACT

The paper defines the conditions for the coefficients of a linear color transformation that guarantee that after one cycle of transformation and inverse transformation all further cycles of transformation do not introduce rounding errors to sample values. Moreover, the upper limits of the rounding error can be calculated according to the formulas given in the paper. The results are very important for nearly lossless compression of color images. Color transformations that decorrelate color components allow a significant increase in compression ratio achieved by use of standard lossless compression techniques applied independently to the components. The results of the paper prove that further cycles of compression and decompression together with color transformations do not increase the rounding errors. The experimental results for the $RGB \rightarrow YC_R C_B$ transformation are also included.

1 INTRODUCTION

Lossless image compression is commonly used in medical imaging as well as for storage and transmission of astronomical and geodetic images. The basic standards for lossless compression of continuous tone images are:

JPEG lossless mode (ISO/IEC IS 10918) [1,2],

JPEG-LS (ISO/IEC IS 14495) [3].

Moreover, it has been proven that for images with limited graylevel range, application of binary image compression standards for coding of bitplanes can be advantageous [6]. The basic binary image compression standard is JBIG (ISO/IEC IS 11544) [4] defining more advanced algorithm than commonly used facsimile recommendations [5].

For the above mentioned techniques, the obtainable compression ratio values are about 2 for natural images. The recently introduced standard JPEG-LS outperforms its predecessor JPEG lossless mode by 20% at most.

Recently, numerous new techniques for lossless compression of grayscale and color images have been developed (see, e.g. [7-11]). The most popular approach comprises differential pulse code modulation with a great variety of more or less sophisticated predictors and variable codeword length encoders.

For its relatively high compression efficiency, the technique known as CALIC (*context-based adaptive lossless/nearly lossless image coding*) [12,13] is considered as a reference technique for research results in lossless image compression. A much simpler algorithm known as LOCO-I (*low-complexity context-based lossless image compression*) [14] has been standardized by ISO as an already mentioned international standard commonly known as JPEG-LS [3]. Employment of the LOCO-I technique leads to slightly lower compression ratios but the difference does not exceed 5% for most of the natural scene and medical images. The consumption of processor time is often even few times lower for the LOCO-I algorithm as compared to the CALIC algorithm.

The principal drawback of lossless techniques is related to modest compression ratios achieved. Recent attempts to overcome this disadvantage did not lead to a turn. Therefore nearly lossless coding has been proposed to trade off between compression ratio and distortion which have to be kept very small [e.g. 3,15,16,17]. Both LOCO-I and CALIC algorithms offer nearly lossless modes of operation. By use of nearly lossless compression methods achievable compression ratio is about 4 to 6 depending on the error limit imposed. A single encoding-decoding cycle results in graceful degradations that are not perceivable. Therefore users are unaware of encoding and decoding an individual image for several times. Nevertheless each encoding-decoding cycle implies new degradations introduced into the image. For example, application of the nearly lossless mode of the LOCO-I algorithm, i.e. the JPEG-LS international standard results often in a loss of 10 dB of the peak signal-to-noise ratio after about 10 cycles of encoding and decoding. Such a situation is absolutely not acceptable in numerous applications where a specialist makes vital decisions by considering images.

2 THE ROLE OF COLOR TRANSFORMATIONS IN IMAGE COMPRESSION

The R , G and B components are highly correlated, therefore their straightforward encoding is not efficient. Decorrelation of components improves the results of further compression. Theoretically optimal is the adaptive Karhunen-Loève transformation, which is rather

sophisticated in application. Employment of the Karhunen-Loève transformation matched to average statistical properties of a whole image leads to results, which are often even poorer than those obtained by usage of $YC_R C_B$ color coordinates [19]. Therefore rough decorrelation of color components is mostly obtained by a linear transformation to the $YC_R C_B$ color space, opponent color space or another similar one. Unfortunately those linear transformations are mostly represented by matrices with noninteger elements. Therefore application of such transformations prior to actual compression leads to some rounding errors. The whole cycle *color transformation – compression – inverse color transformation* is not exactly lossless, i.e. is not exactly reversible.

3 COLOR TRANSFORMATION FOR INTEGER COMPONENT VALUES

It is assumed that an image is represented by R , G and B components. For the sake of brevity let us assume 8-bit representation of component samples. Nevertheless the considerations given below can be adopted for any number of bits of pixel representations. A linear color transformation and the corresponding inverse transformation can be expressed as

$$\begin{bmatrix} D \\ E \\ F \end{bmatrix} = \begin{bmatrix} c_1 \\ c_2 \\ c_3 \end{bmatrix} + \frac{1}{256} \begin{bmatrix} t_{11} & t_{12} & t_{13} \\ t_{21} & t_{22} & t_{23} \\ t_{31} & t_{32} & t_{33} \end{bmatrix} \begin{bmatrix} R \\ G \\ B \end{bmatrix}, \quad (1)$$

$$\begin{bmatrix} R \\ G \\ B \end{bmatrix} = \frac{1}{256} \begin{bmatrix} s_{11} & s_{12} & s_{13} \\ s_{21} & s_{22} & s_{23} \\ s_{31} & s_{32} & s_{33} \end{bmatrix} \begin{bmatrix} D - c_1 \\ E - c_2 \\ F - c_3 \end{bmatrix}, \quad (2)$$

where mostly $c_1 = c_2 = c_3 = 0$. Nevertheless for the $YC_B C_R$ color space, there is $D = Y$, $E = C_B$, $F = C_R$ and $c_1 = 16$, $c_2 = c_3 = 128$ in order to match the dynamic range defined by ITU-R [18].

In order to simplify the considerations and without loss of generality, the equations can be simplified to

$$\begin{bmatrix} D \\ E \\ F \end{bmatrix} = \begin{bmatrix} t_{11} & t_{12} & t_{13} \\ t_{21} & t_{22} & t_{23} \\ t_{31} & t_{32} & t_{33} \end{bmatrix} \begin{bmatrix} R \\ G \\ B \end{bmatrix}, \quad (3)$$

$$\begin{bmatrix} R \\ G \\ B \end{bmatrix} = \begin{bmatrix} s_{11} & s_{12} & s_{13} \\ s_{21} & s_{22} & s_{23} \\ s_{31} & s_{32} & s_{33} \end{bmatrix} \begin{bmatrix} D_1 \\ E_2 \\ F \end{bmatrix}. \quad (4)$$

The RGB samples are integers from the interval [0,255]. Then the RGB values are transformed to a DEF system according to Equation 3. After further lossless encoding and decoding, the D , E and F components have to be converted back to the R , G and B components by use of Eq. 4. The exact R , G and B component values obtained according to Eq. 1 have to be rounded in order to obtain integers D^{rd} , E^{rd} and F^{rd} from the interval [0,255]. Therefore there is

$$\begin{aligned} D^{rd} &= D + \delta_D, \\ E^{rd} &= E + \delta_E, \\ F^{rd} &= F + \delta_F, \end{aligned} \quad (5)$$

There is: $0 \leq |\delta_D|, |\delta_E|, |\delta_F| \leq 0.5$.

Then again the recovered R^d , G^d and B^d samples obtained from Eq. 2 have to be rounded to integers R^{rd} , G^{rd} and B^{rd} from the interval [0,255]. Let us denote:

$$\begin{aligned} \delta_R &= R^{rd} - R, \\ \delta_G &= G^{rd} - G, \\ \delta_B &= B^{rd} - B. \end{aligned} \quad (5)$$

Therefore δ_R , δ_G , δ_B denote the differences between the input R , G , B sample values and those R^d , G^d , B^d rounded after decoding and inverse color transformation. The values δ_R , δ_G , δ_B are integer because R , G , B and R^d , G^d , B^d are also integer.

Proposition 1:

Sample errors δ_R , δ_G , δ_B of the R , G and B components in the first cycle of forward and backward transformations are bounded $|\delta_R| \leq L_R, |\delta_G| \leq L_G, |\delta_B| \leq L_B$,

where

$$\begin{aligned} L_R &= \text{round}[(|s_{11}| + |s_{12}| + |s_{13}|) / 2] \\ L_G &= \text{round}[(|s_{21}| + |s_{22}| + |s_{23}|) / 2] \\ L_B &= \text{round}[(|s_{31}| + |s_{32}| + |s_{33}|) / 2] \end{aligned} \quad (6)$$

Proof:

Equation 4 yields

$$\begin{bmatrix} R^d \\ G^d \\ B^d \end{bmatrix} = \begin{bmatrix} s_{11} & s_{12} & s_{13} \\ s_{21} & s_{22} & s_{23} \\ s_{31} & s_{32} & s_{33} \end{bmatrix} \begin{bmatrix} D + \delta_D \\ E + \delta_E \\ F + \delta_F \end{bmatrix} \quad (7)$$

Equation 4 defines a linear transformation, therefore

$$\begin{aligned} |R^d - R| &\leq |s_{11} \cdot \delta_D| + |s_{12} \cdot \delta_E| + |s_{13} \cdot \delta_F| \\ |G^d - G| &\leq |s_{21} \cdot \delta_D| + |s_{22} \cdot \delta_E| + |s_{23} \cdot \delta_F| \\ |R^d - R| &\leq |s_{31} \cdot \delta_D| + |s_{32} \cdot \delta_E| + |s_{33} \cdot \delta_F| \end{aligned} \quad (8)$$

Relation $|\delta_D|, |\delta_E|, |\delta_F| \leq 0.5$ implies

$$\begin{aligned} |R^d - R| &\leq 0.5 \cdot (|s_{11}| + |s_{12}| + |s_{13}|), \\ |G^d - G| &\leq 0.5 \cdot (|s_{21}| + |s_{22}| + |s_{23}|), \\ |R^d - R| &\leq 0.5 \cdot (|s_{31}| + |s_{32}| + |s_{33}|). \end{aligned} \quad (9)$$

The values of R , G , B are integer, therefore rounding of R^d , G^d and B^d to the nearest integer will result in values R^{rd} , G^{rd} , B^{rd} such that

$$\begin{aligned} |\delta_R| &= |R^{rd} - R| \leq \text{round}[(|s_{11}| + |s_{12}| + |s_{13}|) / 2], \\ |\delta_G| &= |G^{rd} - G| \leq \text{round}[(|s_{21}| + |s_{22}| + |s_{23}|) / 2], \\ |\delta_B| &= |B^{rd} - B| \leq \text{round}[(|s_{31}| + |s_{32}| + |s_{33}|) / 2]. \end{aligned} \quad (10)$$

Q.E.D.

The second cycle of encoding and decoding starts with the component values R^{rd} , G^{rd} , B^{rd} .

Proposition 2:

The conditions:

$$\begin{aligned} (|t_{11}| + |t_{12}| + |t_{13}|) &< 1, \\ (|t_{21}| + |t_{22}| + |t_{23}|) &< 1, \\ (|t_{31}| + |t_{32}| + |t_{33}|) &< 1. \end{aligned} \quad (11)$$

yield the following property:

After the first cycle, all consecutive cycles of forward and backward transformations do not influence the values R^{rd} , G^{rd} , B^{rd} obtained in the first cycle.

Proof:

Equation 3 defines a vector transformation corresponding to the second cycle

$$\begin{bmatrix} R^{rd} \\ G^{rd} \\ B^{rd} \end{bmatrix} \longrightarrow \begin{bmatrix} D^{(2)} \\ E^{(2)} \\ F^{(2)} \end{bmatrix}. \quad (12)$$

The integer components D^{rd} , E^{rd} , F^{rd} obtained in the previous cycle can be transformed according to Equation 4:

$$\begin{bmatrix} D^{rd} \\ E^{rd} \\ F^{rd} \end{bmatrix} \longrightarrow \begin{bmatrix} R^r \\ G^r \\ B^r \end{bmatrix}. \quad (13)$$

Therefore Equation 3 defines the inverse transformation:

$$\begin{bmatrix} R^r \\ G^r \\ B^r \end{bmatrix} \longrightarrow \begin{bmatrix} D^{rd} \\ E^{rd} \\ F^{rd} \end{bmatrix}. \quad (14)$$

There is

$$\begin{aligned} R^{rd} &= R^r - \Delta_R, \\ G^{rd} &= G^r - \Delta_G, \\ B^{rd} &= B^r - \Delta_B. \end{aligned} \quad (15)$$

where $|\Delta_R|, |\Delta_G|, |\Delta_B| \leq 0.5$.

Let us denote

$$\begin{aligned} \Delta_D &= D^{(2)} - D^{rd}, \\ \Delta_E &= E^{(2)} - E^{rd}, \\ \Delta_F &= F^{(2)} - F^{rd}. \end{aligned} \quad (16)$$

Equations (12), (15) and (16) yield the transformation defined by equation 1.

$$\begin{bmatrix} R^{rd} \\ G^{rd} \\ B^{rd} \end{bmatrix} = \left(\begin{bmatrix} R^r \\ G^r \\ B^r \end{bmatrix} + \begin{bmatrix} \Delta_R \\ \Delta_G \\ \Delta_B \end{bmatrix} \right) \longrightarrow \begin{bmatrix} D^{(2)} \\ E^{(2)} \\ F^{(2)} \end{bmatrix} = \left(\begin{bmatrix} D^{rd} \\ E^{rd} \\ F^{rd} \end{bmatrix} + \begin{bmatrix} \Delta_D \\ \Delta_E \\ \Delta_F \end{bmatrix} \right) \quad (17)$$

Therefore (14) implies

$$\begin{aligned} |\Delta_D| &\leq |t_{11}\Delta_R| + |t_{12}\Delta_G| + |t_{13}\Delta_B|, \\ |\Delta_E| &\leq |t_{21}\Delta_R| + |t_{22}\Delta_G| + |t_{23}\Delta_B|, \\ |\Delta_F| &\leq |t_{31}\Delta_R| + |t_{32}\Delta_G| + |t_{33}\Delta_B|. \end{aligned} \quad (18)$$

Therefore

$$\begin{aligned} |\Delta_D| &\leq 0.5(|t_{11}| + |t_{12}| + |t_{13}|), \\ |\Delta_E| &\leq 0.5(|t_{21}| + |t_{22}| + |t_{23}|), \\ |\Delta_F| &\leq 0.5(|t_{31}| + |t_{32}| + |t_{33}|), \end{aligned} \quad (19)$$

Conditions (16) implies that the sample values $D^{(2)}$, $E^{(2)}$, $F^{(2)}$ are rounded to D^{rd} , E^{rd} , F^{rd} which are then transformed back to R^{rd} , G^{rd} and B^{rd} .

Q.E.D.

The latter proposition tells us that further transformation cycles do not introduce additional rounding errors. Thus the errors after several cycles of compression and decompression are the same as those after a single cycle. A good example of a transformation which exhibits the following properties is the transformation $RGB \rightarrow YC_B C_R$.

4 EXPERIMENTAL RESULTS

A series of experiments with a set of histological images has been done. Two of the test images are shown in Fig. 1 and 2.

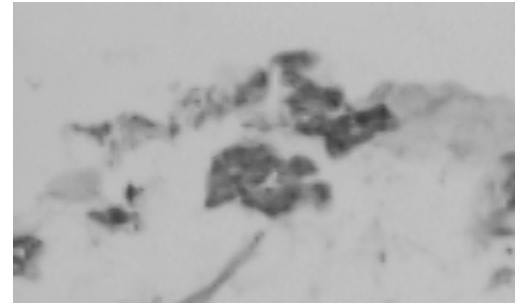


Figure 1. Exemplary test image: *desm1*

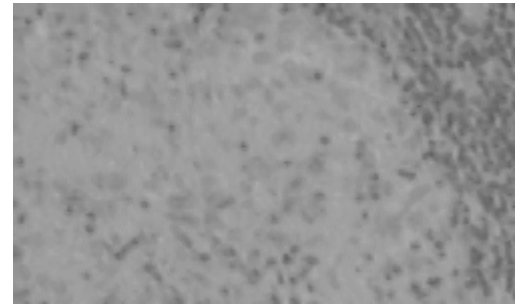


Figure 2. Exemplary test image: *sarco1*

Average compression ratio values for two color spaces are given in Table 1. Lossless compression in the $YC_B C_R$ color space leads to lower compression ratios and better quality than obtained by use of the nearly-lossless mode (Table 2). The limits calculated (Table 3) fit into those set by Proposition 1.

Table 1. Compression ratio for histological images

	LOCO	CALIC
RGB	2.37	2.46
YCBC _R	3.58	3.64

Table 3. Error histograms (as percent) of RGB images after one cycle of color transformations.

Pixel error	R	G	B
0	58.8	72.2	50.2
1	41.2	27.8	49.4
2	0	0	0.4

Table 2. LOCO-I: Comparison of the color transformation technique with nearly lossless mode

Technique	Test image <i>Sarcol</i>							Test image <i>Desm1</i>						
	Kr	δ_{\max}			PSNR[dB]			Kr	δ_{\max}			PSNR[dB]		
		R	G	B	R	G	B		R	G	B	R	G	B
Lossless with color transformation	3.03	1	1	2	51.8	54.0	51.0	3.88	1	1	2	52.0	54.0	50.9
Nearly lossless with $\delta_{\max} = 1$	3.10	1	1	1	49.9	49.8	49.8	4.71	1	1	1	49.9	50.0	49.9
with $\delta_{\max} = 2$	4.01	2	2	2	45.1	45.1	45.1	6.47	2	2	2	45.6	45.5	45.4
with $\delta_{\max} = 3$	4.73	3	3	3	42.2	42.1	42.1	8.09	3	3	3	42.9	42.8	42.7

5 CONCLUSIONS

The paper defines the conditions for the coefficients of a linear color transformation that guarantee that after one cycle of transformation and inverse transformation all further cycles of transformation do not introduce rounding errors to sample values. Moreover, the upper limits of the rounding error can be calculated according to the formulas given in the paper. The results are very important for nearly lossless compression of color images.

The results of the paper prove that further cycles of compression and decompression together with color transformations do not increase the rounding errors if the conditions of Proposition 2 are fulfilled. In the case of nearly lossless techniques the errors increase in each cycle of coding and decoding.

References

- [1] ISO/IEC IS 10918-1 / ITU-T Rec. T.81, "Information technology – digital compression and coding of continuous-tone still images: requirements and guideline."
- [2] W. B. Pennebaker, J. L. Mitchell, JPEG still image compression standard, New York, Van Nostrand Reinhold 1993.
- [3] ISO/IEC DIS 14495, "Lossless and near-lossless compression of continuous-tone still images."
- [4] ISO/IEC IS 11544 / ITU-T Rec. T.82, "Coded representation of picture and audio information – progressive bi-level image compression".
- [5] ITU-T Rec. T.4, "Standardization of group 3 facsimile apparatus for document transmission".
- [6] R. Arps, T. Truong, "Comparison of international standards for lossless still image compression", Proc. IEEE, 1994, 82, s. 889-899.
- [7] V.K. Heer, H.E. Reinfelder, "A comparison of reversible methods for data compression", Proc. SPIE, vol. 1233, Medical Imaging IV, 1990, pp. 354-365.
- [8] N.D. Memon, K. Saywood, "Lossless image compression: a comparative study", Proc. SPIE, vol. 2418, 1995, pp. 8-20.
- [9] S. Wong, L. Zaremba, D. Gooden, H.K. Huang, "Radiologic image compression - a review", Proc. IEEE, vol. 83, 1995, pp. 194-219.
- [10] G. Yovanof, J. Sullivan, "Lossless predictive coding of color graphics", Proc. SPIE, vol. 1657, Image Processing Algorithms and Techniques, 1992, pp. 68-82.
- [11] B. Meyer, P. Tischer, "TMW - a new method for lossless image compression", 1997 Picture Coding Symposium, Berlin, VDE 1997, s. 533-538.
- [12] X. Wu, N. Memon, "Context-based adaptive lossless codec", IEEE Trans. Communications, vol. 45, 1997, pp. 437-444.
- [13] X. Wu, "Lossless compression of continuous-tone images via context selection, quantization, and modeling", IEEE Trans. Image Processing, vol. 6, 1997, pp. 656-664.
- [14] M.J. Weinberger, G. Seroussi, G. Sapiro, "LOCO-I: a low complexity lossless image compression algorithm", Proc. IEEE Data Compression Conf., New York, 1996.
- [15] L. Ke, M.W. Marcellin, "Near-lossless image compression: minimum-entropy, constrained-error DPCM", IEEE Trans. Image Processing, vol. 7, 1998, pp. 225-228.
- [16] M. Hasegawa, S. Kato, Y. Yamada, "Lossless and scalable coding scheme of super high definition images", Proc. Picture Coding Symposium 1999, Portland OR, pp. 127-131.
- [17] K. Chen, T.V. Ramabadran, "Near-lossless compression of medical images through entropy-coded DPCM", IEEE Trans. Medical Imaging, vol. 13, 1994, pp. 538-548.
- [18] ITU-R Rec. BT.601-4, Encoding parameters of digital television for studios.
- [19] G. Yovanof, J. Sullivan, "Lossless predictive coding of color graphics", Proc. SPIE, vol. 1657, Image Processing Algorithms and Techniques, 1992, pp. 68-82.